High Extinction Ratio And Saturation Power Traveling-Wave Electroabsorption Modulator

Yi-Jen Chiu, Hsu-Feng Chou, Volkan Kaman, Patrick Abraham, and John E. Bowers

***Abstract*—An InGaAsP multiquantum-well traveling-wave electroabsorption modulator is demonstrated with high extinction ratio and modulation efficiency. By designing a strain-compensated quantum-well active region with traveling-wave design, high saturation power (>14 dBm) for >20-GHz high-speed performance (1.5 dB drop at 20 GHz) is achieved. Due to high modulation efficiency (> 30 dB/V for 0 to 1 V 40-dB extinction ratio in 2 V), error free 10-Gb/s operation with 1 V_{p-p} driving voltage is obtained. By comparing codirections and counterdirections of optical and microwave interactions, pulse generation at 40 GHz shows that the traveling-wave performance has an advantage for short pulse with high-power output, where pulsewidth of as short as 4.5 ps is obtained in this kind of devices.**

***Index Terms*—Electroabsorption, high extinction ration, high saturation power, high speed, low driving voltage, modulator, traveling wave.**

I. Introduction

ELECTROABSORPTION MODULATORS (EAM) have been widely used for optical fiber communication due to their low chirp and integration with other semiconductor devices. High bit rates in both optical time-division-multiplexing (OTDM) and wavelength-division-multiplexing (WDM) systems have imposed stringent demands on EAM's performance, such as high modulation ratio with low driving power, high saturation power and high bandwidth. There are generally two ways to achieve these requirements: improving the material in the active regions and increasing the device lengths. In the former, there are several reports on the improvement of high efficiency and power [1]–[4] by increasing the quantum-well (QW) number or thickness to get sensitive modulation with applied voltage and reducing the band offset of QW against the barrier. In the later longer devices have longer electroabsorption interaction and larger absorption volume, thus the modulation efficiency and saturation power can be improved [5], [6]. However, the conventional RC-lumped element design inevitably limits the device bandwidth, and also the tolerance on the design of the active region [7], [8]. Recently, traveling-wave EA modulators (TWEAM) have been demonstrated to overcome the RC-limitation [9]–[11]. In this work, based on improving the active region from previous work [9], we fabricated multiple-quantum-well (MQW) TWEAMs to further enhance the modulation efficiency, high saturation power and speed. By comparing codirections and counterdirections of optical and microwave interaction, 40-GHz sinusoidal driven optical pulses for codirection configuration exhibits higher output power, indicating that the distributed effect dominates the performance and the traveling wave can have an advantage to get high-power high-extinction ratio and short pulses.

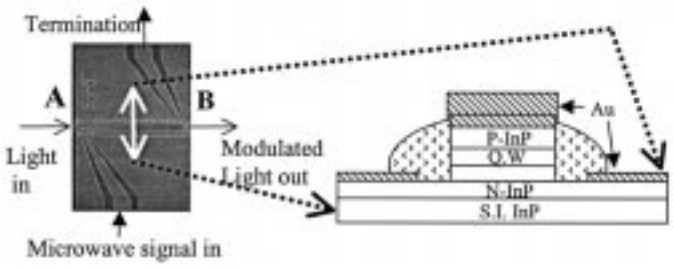

Fig. 1. The top view (top) and the schematic cross section (bottom) of TWEAM. The points A and B represent two different directions of launching optical power (codirection and counterdirection).

II. Device Fabrication

The epilayer used for the TWEAM is an InGaAsP-based material grown by MOCVD on a semi-insulated InP substrate. Wider wells and lower barriers than the previous work [9] were designed and grown to improve the quantum-confined-Stark effect and to reduce the bandgap offset [1], [2]. Furthermore, a longer device than [9] is designed to get higher tolerance on the design of active region. The active region consists of 10 tensile-strain wells (InGaAsP, 0.35%, 120 nm) and 11 compressive-strain barriers (InGaAsP, 0.57%, 70 nm). Cladding layers of p-InP (top) and n-InP (bottom) are grown and sandwich the active region. The total thickness of the intrinsic region is about 300 nm. As shown in Fig. 1, a 330-μm long and 2-μm-wide buried ridge-waveguide device is fabricated, where the ridge is formed by CH_4–H_2–Ar reactive-ion-etching (RIE). PMGI is utilized for passivating the etching surface and bridging the metal. Two coplanar waveguides (CPW) lines forming the traveling-wave circuit are used for the microwave power feed and load line.

III. Experiments Results and Discussion

Fig. 2 shows the normalized lens-coupled fiber-to-fiber transmission measurement (TM-mode) as function of bias for an optical power of 2 dBm at a wavelength of 1555 nm. The insertion

Manuscript received November 20, 2001; revised February 25, 2002.

Y.-J. Chiu, H.-F. Chou, and J. E. Bowers are with the Department of Electrical and Computer Engineering, University of California, Santa Barbara, Santa Barbara, CA 93106 USA (e-mail: chiu@opto.ucsb.edu).

V. Kaman was with the Department of Electrical and Computer Engineering, University of California, Santa Barbara, Santa Barbara, CA 93106 USA. He is now with Calient Inc., Goleta, CA 93117 USA.

P. Abraham was with the Department of Electrical and Computer Engineering, University of California, Santa Barbara, Santa Barbara, CA 93106 USA. He is now with Agility Communications, Goleta, CA 93117 USA.

Publisher Item Identifier S 1041-1135(02)04077-6.

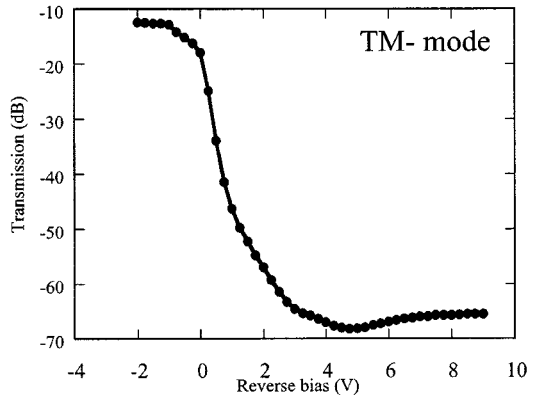

Fig. 2. The fiber-to-fiber optical transmission with bias.

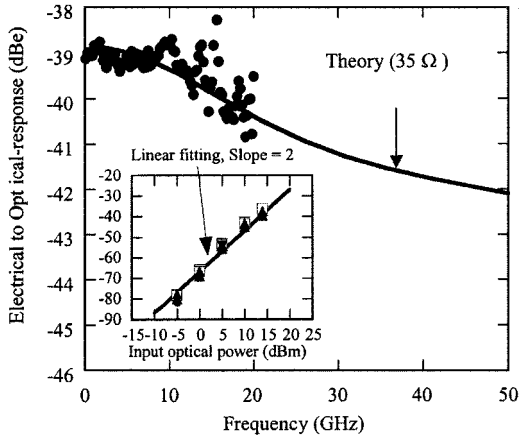

Fig. 3. The frequency response for theoretical curve (solid line) and the experiment curve (points). The electrical-to-optical response is defined as The insert is the plot of the relative EO response with input optical power at the frequencies of 0.13, 2.5, 5, 10, 12.5, 15, 17.5, and 20 GHz, while the line is a linear fit with slope = 2. The device is biased at $\mathrm{Vbias} = 0.4$ V.

loss at dc is about −12 dB at forward bias −1 V. The total coupling loss for both facets is about −5 to −6 dB. As shown in Fig. 2, a total extinction ration of 57 dB (from −1 to 4.5 V) is achieved. It should be noted that the modulation efficiency is higher than 30 dB/V for 0 to 1 V, while the modulation depth is 40 dB for the bias from 0 to 2 V. High extinction ratio driven by lower swing voltage than [9] is mainly attributed to the improved active region.

The frequency response was measured by a HP Lightwave Component Network analyzer (HP8703A). The device was terminated by a 35-Ω chip resistance with ribbon bonding for obtaining broadband response. As shown in Fig. 3, a flat electrical-to-optical (EO) response was obtained with 1.5-dB drop at 20 GHz. The EO response is defined as $20 \cdot \log(P_o(W)/I_e(A) \cdot 1(A/W))$, where P_o is output optical power, I_e is the input electrical current, and the coversion efficiency of photoreceiver is relative to 1 A/W. The device is biased at $\mathrm{Vbias} = 0.4$ V. The distributed model [12] (solid curve in Fig. 3) was used to fit the experiment results, where the expected 3-dB bandwidth is about 40 GHz. The microwave characteristics used in this model for this calculation are extracted from the S-parameters measurements on the straight waveguides [15]. Better microwave attenuation (0.2 dB/100 μm at 20 GHz) and flatter frequency response

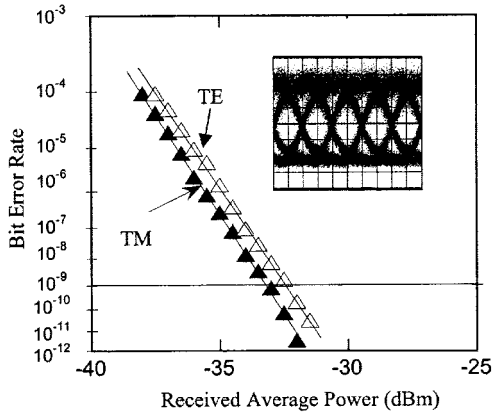

Fig. 4. 10-Gb/s bit-error-rate transmission with received power. The eye diagram is shown in the insert.

than [9] is mainly attributed to decreasing the parasitic capacitance on the waveguide.

In order to examine the capability of handling the input optical power, high-speed modulation is measured against the estimated different power levels into device (−5, 0, 5, 10, and 14 dBm). The insert of Fig. 3 shows the relative EO response as function of input optical power, while the data points are chosen at frequencies of 0.13, 2.5, 5, 10, 12.5, 15, 17.5, and 20 GHz. Similar responses (transfer function) as Fig. 3 for different pumping levels are obtained, while the measured data was within 2 dB for each level. The 2-dB penalty is mainly due to the fluctuation from instrument at high frequency (shown in Fig. 3). The relation of the EO response and the input power is linear with slope of two, suggesting that there are no significant degradation (within 2 dB) of frequency response associated with the effects of electron-hole pile-up [10] or the photocurrent effect on the high optical power excitation [14]. Because of the high optical loss of this device, the EO response is low (insert of Fig. 3). However, it can be improved by high optical input power.

A 10-Gb/s data transmission was performed to test the device performance. As shown in Fig. 4, for a pattern length of $2^{31}-1$ error free operation was achieved with a receiver sensitivity of −32.5 dBm for TE and −33.3 dBm for TM. Due to the high modulation efficiency, successful transmission was achieved with 1 Vp-p driving voltage for both polarization states. The reason for the 0.8-dBm polarization penalty is that the modulation efficiency for TE mode is lower.

To further investigate the traveling-wave structure sinusoidal driven optical short pulses were generated to test the device [6]. Two configurations of measurement were compared: reference one is the codirection case in which the direction of launching optical wave (from A to B in Fig. 1) is the same as the microwave, the other configuration is the reverse, the counterdirection case. The two CPW lines of the device were connected by two high-bandwidth (>40 GHz) probes, while one is terminated by a 50-Ω resister, and the other was connected by a 40-GHz sinusoidal electrical signal with $V_{p-p} = 5.6$ V (measured by a 50-Ω load). The optical power is 2 dBm at the wavelength of 1555 nm. The output optical pulses were amplified by erbium-doped fiber amplifiers (EDFAs) and then sent to autocorrelator for measuring pulsewidths.

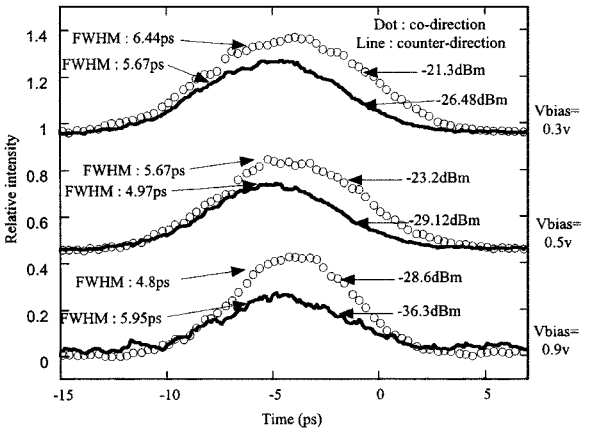

Fig. 5. The autocorrelator traces of codirections and counterdirections for different bias. As $\mathrm{bias} = 0.9$ V, the power of counterdirection is so low that the pulse need be taken by higher scale than codirection.

TABLE I
THE SUMMARIES OF OPTICAL PULSES SHOWN IN FIG. 5

Bias (v)	Power (dBm) Co-/Counter- direction	Pulse width (ps) Co-/Counter- direction
0.3	-21.3 / -26.48	6.44/5.67
0.5	-23.2 / -29.12	5.67/4.97
0.7	-25.4/-32.4	5.04/4.83
0.9	-28.6 / -36.3	4.8/5.95
1	-30.8 / ?	4.5 / ?

Fig. 5 plots the autocorrelated pulses for biases 0.3, 0.5 and 0.9 V, while Table I summarizes the output power (before being amplified by EDFAs) and pulsewidths of full-width at half-maximum (FWHM) for different biases. The amplitudes and output power of codirection pulses are significantly higher than those of the counterdirection. As seen in Table I, increasing the bias causes larger differences, specifically, the power penalty due to counterdirection reaches as high as 8 dB when the bias is 0.9 V. Both counterdirection and codirection measurements are the same if this were a lump element. However, the change in the output power indicates that the electroabsorption interaction in this device can only be explained by distributed effects along the long waveguide. Two main factors effect the output optical power and pulsewidths are the walkoff time and the time-gating window distributively generated by the microwave wave along the waveguide. The waveguide length is about 1/5 of microwave wavelength (index ~ 5.5 at 40 GHz), implying that the propagation wave behavior can not be neglected. Because the electrooptical interaction happens in the sharp ON–OFF modulation regime ($\mathrm{Vbias} = 0$ to 2 V in Fig. 2), the time-switching window becomes narrower as the bias increases, therefore the output optical pulses are very sensitive to the walkoff time relative to the microwave [12]. Obviously, the higher walkoff for the counterdirection case than the codirection case would result in the lower output power. And the pulses might be shortened by deteriorated the average optical power. At lower bias (< 0.7 V) narrower pulses are observed in counterdirection. Due to the time-switching window changes with the bias, as can been seen in Table I, the pulses for the counterdirection becomes wider as bias >0.7 V. In the extreme case, when biased at 1 V, the output power for the counter-direction case is so small that the autocorrelated trace cannot be measured, while the optical pulse width of 4.5 ps ($\mathrm{bias} = 1$ V) was achieved in the codirection case.

IV. CONCLUSION

In summary, we have successfully fabricated a high-modulation-efficiency and higher saturation power traveling-wave InGaAsP-EA modulator. As high as 40 dB (within 2 V) of modulation depth and higher than 30 dB/V (0 V to 1 V) of modulation efficiency are demonstrated. The -3-dB bandwidth is higher than 20 GHz (about -1.5-dB drop at 20 GHz) for 330-μm-long waveguide. High-speed measurement under high-power excitation shows no power saturation up to excitation power of 14 dBm. Due to the sharp modulation depth, a 10-Gb/s data was successfully transmitted (sensitivity -33.3 dBm) for low driving power of 1 V_{p-p}. The traveling-wave performance is also manifested by launching optical power with codirection and counterdirection with respect to the microwave. Extreme difference between these two configurations suggests that distributed effects dominate device performance.

REFERENCES

[1] A. M. Fox, D. A. B. Miller, G. Livescu, J. E. Cunningham, and W. Y. Jan, "Quantum well carrier sweep out: Relation electroabsorption and exciton saturation," *IEEE J. Quantum Electron.*, vol. 27, pp. 2281–2295, Oct. 1991.

[2] G. Bastard, E. E. Mendez, L. L. Chang, and L. Esaki, "Variational calculations on a quantum well in an electric Physical Review B," *Condensed Matter*, vol. 28, pp. 3241–3245, Sept. 1983.

[3] A. Ougazzaden and F. Devaux, "Strained InGaAsP/InGaAsP/InAsP multi-quantum well structure for polarization insensitive electroabsorption modulator with high power saturation," *Appl. Phys. Lett.*, vol. 69, pp. 4131–4132, Dec. 1996.

[4] F. Devaux, J. C. Harmand, I. F. L. Dias, T. Guettler, O. Krebs, and P. Voisin, "High power saturation, polarization insensitive electroabsorption modulator with spiked shallow wells," *Electron. Lett.*, vol. 33, pp. 161–163, Jan. 1997.

[5] D. D. Marcenac, A. D. Ellis, and D. G. Moodie, "80 Gbit/s OTDM using electroabsorption modulators," *Electron. Lett.*, vol. 34, pp. 101–103, Jan. 1998.

[6] V. Kaman, Y.-J. Chiu, T. Liljeberg, S. Z. Zhang, and J. E. Bowers, "Integrated tandem traveling-wave electroabsorption modulators for >100 Gbit/s OTDM applications," *IEEE Photon. Technol. Lett.*, vol. 12, pp. 1471–1473, Nov. 2000.

[7] R. Weinmann, D. Baums, U. Cebulla, H. Haisch, D. Kaiser, E. Kuhn, E. Lach, K. Satzke, J. Weber, P. Wiedemann, and E. Zielinski, "Polarization-independent and ultra-high bandwidth electroabsorption modulator in multiquantum-well deep-ridge waveguide technology," *IEEE Photon. Technol. Lett.*, vol. .8, pp. 891–893, July 1996.

[8] G. E. Shtengel, A. E. Bond, Y. A. Akulova, and C. L. Reynolds, Jr., "High-speed InGaAsP electroabsorption modulators: Dependence of the device characteristics on the mesa design," in *Optical Fiber Communication Conf. Tech. Dig. Postconf. Edition*, 2000, vol. 4, pp. 120–122.

[9] S. Z. Zhang, Y.-J. Chiu, P. Abraham, and J. E. Bowers, "25GHz polarization-insensitive electroabsorption modulators with traveling-wave electrodes," *IEEE Photon. Technol. Lett.*, vol. 11, pp. 191–193, Feb. 1999.

[10] G. L. Li, S. A. Pappert, P. Mages, C. K. Sun, W. S. C. Chang, and P. K. L. Yu, "High-saturation high-speed traveling-wave InGaAsP–InP electroabsorption modulator," *IEEE Photon. Technol. Lett.*, vol. 13, pp. 1076–1078, Oct. 2001.

[11] S. Irmscher, R. Lewen, and U. Eriksson, "Influence of electrode width on high-speed performance of traveling-wave electroabsorption modulators," in *2001 International Conf. Indium Phosphide and Related Materials*. Piscataway, NJ: IEEE, 2001, pp. 436–439.

[12] Y.-J. Chiu, V. Kaman, S. Z. Zhang, and J. E. Bowers, "Distributed effects model for cascaded traveling-wave electroabsorption modulator," *IEEE Photon. Technol. Lett.*, vol. 13, pp. 791–793, Aug. 2001.

[13] M. Suzuki, H. Tanaka, and S. Akiba, "High-speed characteristics at high input optical power of GaInAsP electroabsorption modulators," *Electron. Lett.*, vol. 24, pp. 1272–1273, Sept. 29, 1988.

[14] G. L. Li, W. X. Chen, P. K. L. Yu, C. K. Sun, and S. A. Pappert, "The effects of photocurrent on microwave properties of electroabsorption modulators," in *1999 IEEE MTT-S International Microwave Symposium Dig.*, vol. 3, pp. 1003–1006.

[15] P. A. Rizzi, *Microwave Engineering Passive Circuits*. Englewood Cliffs, NJ: Prentice Hall, 1988.